Modern Method of Ultimate Strength Analysis of Offshore Structures†

Yukio UEDA* **and Sherif M. H. RASHED****

Abstract

Evaluation of ultimate strength and history of collapse of structures in their intact and damaged conditions is one of the key issues in advanced design techniques based on explicit safety evaluation and collective optimization. This paper describes an efficient method, the Idealized Structural Unit Method, to evaluate ultimate strength of structures. Its application to offshore frame structures is presented taking account of the nonlinear behavior of members, joints and the structure as a whole. Methods to account for strain hardening, damage effects and local shell buckling are summarized. Examples are presented to demonstrate the accuracy and efficiency of this method.

KEY WORDS : (Ultimate strength) (Idealized Structural Unit Method) (Tubular element) (Joint model) (Dent) (Damage) (Strain hardening)

1. Introduction

Traditionally, structural design has been based on providing a higher structural capacity at first failure (such as buckling or yielding) than the anticipated load multiplied by a certain factor of safety. Loads considered are those of frequent occurrence, while extreme loads are not explicitly dealt with. Safety has been taken into account implicitly based on the value of the factor of safety and past experience with similar structures.

With the trend towards building ever larger structures and devising different structural layouts to suit new types of structures in different environments, safety could not be evaluated based on solely past experience. An explicit consideration of safety is needed for such structures. At present, two main streams of safety assessment may be recognized. A deterministic approach, where ultimate strength of the structure (as designed) is compared to the extreme load expected during the lifetime of the structure; and a statistical approach aiming to estimate the probability of collapse. In both approaches, evaluation of ultimate strength under certain circumstances is one of the key issues to be considered.

Many designers also show a great interest in the history of collapse in order to design efficient layouts of structural members with ample redundancy.

Effects of damage, in the form of fatigue cracks or deformation caused by accidental loads (such as dents on offshore structures caused by collision) are also gaining a lot of attention ; not only for the purpose of evaluating the safety and serviceability of a damaged structure, but also for integrated design/inspection/repair optimization at the design stage. Here also, evaluation of ultimate strength of the structure in such damaged conditions is an essential step in this context.

In evaluating the ultimate strength, the "collapse mechanism method" [1] has been successfully used, specially with frame structures. It has been also extended to statistical assessment of safety [2, 3]. The method is simple and only ultimate strength of individual structural members is required. However, it sometimes turns out to be a very lengthy procedure due to the large number of mechanisms to be considered. This method is limited to structures which do not show significant large displacement effects and do not provide any information on the history of collapse.

A general reliable theoretical approach to ultimate strength must take into account the effect of plasticity and large displacement not only on strength, but also on stiffness of individual structural members. Such local failures as buckling or plasticity may cause redistribution of the internal forces and a structure may display a highly nonlinear behavior until its ultimate collapse.

Although analytical solutions may be obtained in very simple cases, for more realistic structures, numerical methods, especially the finite element method is a very powerful tool. However, the limits of cost associated with data preparation and computer time restrict the size of

† Received on May 7, 1990

* Welding Research Institute Osaka University

** MSC Japan LTD. Kansai Branch

Transactions of JWRI is published by Welding Research Institute of Osaka University, Ibaraki, Osaka 567, Japan

problems to be handled. Error control is difficult and it requires long personal experience in order to reduce the risk of misleading results.

In order to overcome some of these difficulties with offshore braced frames, many brace models have been proposed. According to Zayas [4], they may be classified into two groups. The first is the "physical theory brace models" presented by Higginbotham [5], Nilforoushan [6] and Singh [7]. They used a pin-ended model with equivalent effective length and a plastic hinge at the center. The analytical formulations are based on assuming an axial force-moment interaction curve and an elasto-perfectly-plastic moment-curvature relationship at the center hinge. The second group is the "phenomenological brace models". The basis of these models is to pre-define the shape of the axial force-axial displacement response of a truss element representing the brace by employing either mathematical or empirical results. Models of this type have been developed by Higginbotham [5], Nilforoushan [6], Singh [7], Marshall [8], Roeder [9], Jain [10] and Maison [11]. In these models, however, only the axial force acting on the member is considered. End moments and/or lateral load are not taken into account. These, in many cases, have a large effect on buckling and post-buckling behavior of braces.

For efficient, accurate and reliable analysis of large size structures of various types, the authors, in 1974, proposed a new method of nonlinear analysis [12, 13], which has later been named the Idealized Structure Unit Method (ISUM) [14], using large structural units as elements and representing their idealized elastic large deflection behavior in concise analytical-numerical forms and taking account of plastic behavior with the aid of the plastic node method [15, 16].

The ISUM has been successfully applied to ultimate strength analyses of transverse rings [12, 13] and decks [17, 18] of a tanker, double bottom structures [14], and offshore structures [19, 20]. At present several elements have been developed, such as deep girders [12, 13], rectangular plates [14, 17], stiffened plates [18], tubular members [19-25] with particular features and joint models [26].

In this paper, application of ISUM to offshore structures is described introducing several idealized tubular members [19-25] and joint models [26].

2. Outline of the Idealized Structural Unit Method

In the ISUM, a structure is divided into a relatively small number of elements. An element is taken as the largest possible structural unit. Each element should have a limited number of nodal points where the least required number of degrees of freedom is provided. Such elements may be grouped according to their type. These types are few for a specified type of structures, such as jack-up rigs, jackets etc. Under an increasing load, each type of elements exhibits complicated nonlinear behavior. Therefore, the behavior of each type of these structural units is investigated based on fundamental theories, refined theoretical analysis such as a finite element analysis and/or experimental studies. The behavior is then idealized and conditions are formulated for all possible or expected failures in an element, such as buckling of some components of the element and/or yielding of some areas, etc. Stiffness matrices are also derived in each stage of nonlinear behavior, i. e. before any failure and after different combinations of failures.

Once establishing failure conditions and deriving incremental stiffness matrices for various types of such large elements and keeping them ready for use, various types of structures may be readily modeled and easily analyzed.

The incremental method is suitable for this nonlinear analysis. At any loading level, knowing the state of failures of each element, the corresponding incremental stiffness matrix can be selected. The assembly of the stiffness matrices of all elements yields overall stiffness matrix of the structure.

Under the appropriate boundary conditions, a load increment may be applied, the corresponding structural response may be determined and the state of failures is examined in each element. The coordinates of nodal points, and stiffness matrices of the elements may then be updated and load increments may be applied until the structure shows its ultimate strength.

3. Outline of Nonlinear Behavior of Offshore Tubular Space Frames

Offshore tubular space frames are usually constructed of several tubular chords (legs) braced by a large number of tubular bracing members. A member running between two joints is usually a prismatic circular tube. The thickness of the members is sometimes increased locally at the joints to increase their strength.

When an offshore structure of this type is exposed to extreme loads, structural members exhibit very highly nonlinear behavior. Many researchers have investigated this highly nonlinear behavior of tubular members, considered as beam-columns [27-34].

Based on these studies, an outline of the no linear behavior of these tubular structural members is described.

When a tubular member is subjected to an increasing load, various types of failures may take place depending on the dimensions and material of the member, its boundary condition and the ration of the load components.

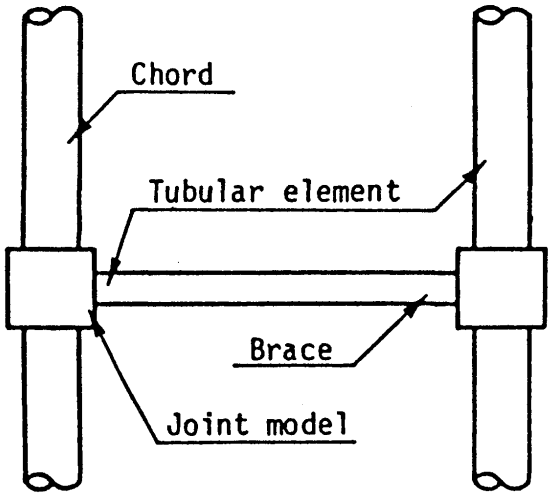

Fig. 1 Tubular element and joint model in offshore structure.

If the member wall is thick enough, no local shell buckling of the tube wall may take place under compression [31]. When such a tube of high or medium slenderness ratio is subjected to a load combination with dominating axial compression, it exhibits a failure free behavior until overall elastic or elastic-plastic buckling occurs. In this case, plastic hinges are formed at the regions of maximum bending moments (midspan and fixed or restrained ends). A tube with lower slenderness ratio does not buckle and it shows its fully plastic strength, irrespective of the type of loading.

Thinner tubes may exhibit local shell buckling before or after the overall buckling.

When bending moment and/or distributed loads are pronounced, the tube tends to deflect laterally so as to produce plastic hinges. Once a plastic hinge is formed, the internal forces must satisfy the condition of plastic strength (with or without strain-hardening effect), but the combination of internal forces may change. The structure with such plastic hinges may sustain further load increments until the structure collapses plastically forming a mechanism with a sufficient number of plastic hinges induced, or when successful internal force redistribution can not be achieved.

In a tubular frame with simple (unstiffened) joints, joints may exhibit considerable flexibility in the elastic as well as the elastic-plastic ranges. Some joints may reach their ultimate strength. These may cause excessive deflections and different internal force distribution in the structure.

In the analysis, the structure may be modeled as a group of prismatic tubular members, modeled by "tubular elements", and joint cans, modeled by "joint elements", as shown in **Fig. 1**.

The behavior of an element, before and after failures,

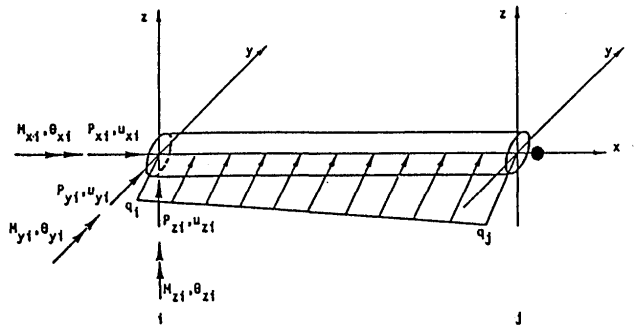

Fig. 2 The tubular element.

may be expressed by the relationship between the nodal force vector and the nodal displacement vector. Since the behavior is nonlinear, the incremental procedure is used in this method.

4. Idealized Tubular Structural Unit [19]

4. 1 Elastic stiffness matrix

For a tubular element, if a conventional displacement function, such as a polynomial of 3rd order is adopted, the geometrical nonlinearity, such as buckling, large displacement, may not be taken into account with sufficient accuracy unless the tubular member is divided into many small elements. Naturally, this causes enormous increase of the total number of degrees of freedom.

In order to deal accurately with the geometrical nonlinearity using one element to model one whole member, a sophisticated displacement function should be employed. Here, the tubular element is dealt with as a beam-column.

An element is considered to be subjected to nodal force $\{R\} = [R_i \ R_j]^T$ and a linearly distributed lateral load q as shown in **Fig. 2**. Six degrees of freedom are considered at each nodal point i and j. Nodal displacement and force vectors, $\{U\}$ and $\{R\}$ may be expressed as

$$\{U\} = [U_i \ U_j]^T, \quad \{R\} = [R_i \ R_j]^T, \tag{1}$$

where
$$\{U_i\} = [U_{xi}, \ U_{yi}, \ U_{zi}, \ \theta_{xi}, \ \theta_{yi}, \ \theta_{zi}]^T$$
$$\{U_j\} = [U_{xj}, \ U_{yj}, \ U_{zj}, \ \theta_{xj}, \ \theta_{yj}, \ \theta_{zj}]^T$$
$$\{R_i\} = [P_{xi}, \ P_{yi}, \ P_{zi}, \ M_{xi}, \ M_{yi}, \ M_{zi}]^T$$
$$\{R_j\} = [P_{xj}, \ P_{yj}, \ P_{zj}, \ M_{xj}, \ M_{yj}, \ M_{zj}]^T$$
$$[\ ]^T = \text{transposed matrix of } [\ ]$$

Before buckling or yielding takes place, the behavior of the structural unit dealt with as a beam column may be expressed by the following differential equation :

$$\frac{d^4w_y}{dx^4} + k^2\frac{d^2w_y}{dx^2} = \frac{l}{EI}q_y$$
$$\frac{d^4w_z}{dx^4} + k^2\frac{d^2w_z}{dx^2} = \frac{l}{EI}q_z \qquad (2)$$

where w_y and w_z = lateral deflections in the xy and zx planes

$k = \sqrt{P/EI}$ is a common variable in the two equations

P = internal axial force

E = Young's modulus

I = cross-sectional moment of inertia

q_y and q_z = components of the lateral load q in y and z directions

The above two equations may be solved independently. When the internal axial force P is compressive (positive), the general solution of the first part of Eq. (2) may be written as

$$w_y = a\cos kx + b\sin kx + cx + d + f(q_y) \qquad (3)$$

$f(q_y)$ is dependent on the distribution of the lateral load q_y. The constants of integration a, b, c and d are determined from the boundary conditions at nodal points i and j, in terms of the nodal displacement $\{U\}$. Based on this displacement function, the relationship between nodal force $\{R\}$ and nodal displacement $\{U\}$ may be obtained, using the following relations.

The bending moment M_z and axial force P_x may be expressed as

$$M_z = -EId^2w_y/dx^2 \qquad (4)$$
$$P_{xi} = -P_{xj} = EA(u_{xi} - u_{xj} - u_b)/L \qquad (5)$$

where u_b = the axial shortening due to bending of the element (see Appendix I)

Neglecting small terms of higher order, an increment of the nodal force $\{dR\}$ may be expressed as follows.

$$\{dR\} + \{dQ\} = [K]\{dU\} \qquad (6)$$

where $[K]$ = the tangential stiffness matrix

$\{dQ\}$ = a load vector associated with the distributed load applied on the element

The explicit forms of $[K]$ and $\{dQ\}$ are given in Appendix I.

When the internal axial force is tensile (negative) the same $[K]$ and $\{dQ\}$ are obtained in which k in a_1 and a_2 (See Appendix I) is replaced by $k^* = \sqrt{|P|/EI}$.

It is to be noted that the effect of the lateral load appears not only in $\{dQ\}$, but also in $[K]$. Here, the exact solution, Eq. (3), of the large deflection differential equations is employed as the displacement function of the element. Accordingly, the effect of elastic large deflection is taken into account.

4.2 Ultimate Strength of Tubular elements [19]

The nodal force-displacement relationship, Eq. (6) holds until the element buckles and/or yielding starts. After yielding has started, even locally, the stiffness of the element decreases. However, Eq. (6) is assumed to hold in the analysis until the element buckles, or one or more full plastic cross sections are developed.

In the following, the conditions of the buckling strength and the full plastic strength of a cross section are represented and the ultimate strength condition is constructed as the combination of these.

Buckling Strength.

Since one member is modeled by one element, initial out-of-straightness and residual stresses may not be explicitly considered. These have no effect on full plastic strength of cross-sections. However they have an effect on buckling strength, which may be taken into account by using a suitable column curve.

From numerous reports on column strength, suitable column curves may be selected. In this study, one of those presented in Ref. [32] is used. The buckling condition is then derived in terms of a buckling function Γ_B as

$$\Gamma_B = P - P_B = 0 \qquad (7)$$

Short columns may attain their full plastic axial compressive strength P_P without buckling. The above equation in this case may be rewritten as,

$$\Gamma_B = P - P_P = 0 \qquad (7')$$

Effective Length for Buckling.

In the case of three dimensional frame structures, determination of the plane of minimum restraint and the buckling configuration requires a complicated and time consuming process. However, the restraining stiffness at nodal points i and j about y and z axes may be obtained from the global tangential stiffness matrix and the restraining stiffness at i and j and then the effective buckling length may be determined [34].

Full Plastic Strength.

As the effect of shearing stresses on plastic strength is assumed to be negligible, the internal shearing forces P_y

and P_z, and the internal twisting moment M_x do not affect the full plastic strength interaction relationship. This is expressed by the full plastic function Γ_P as,

$$\Gamma_P = (\,|\sqrt{M_y^2 + M_z^2}\,|M_P) - \cos\pi\ |\,P\,|\,/2P_p = 0 \tag{8}$$

where M_P = the full plastic bending moment of the cross-section

P_P = the full plastic axial force of the cross-section

Equation (8) may be represented as shown in **Fig. 3**.

Ultimate Strength Interaction Relationship.

Depending on the mechanical properties of the element and the nature of the increasing load vector applied on it, it reaches the ultimate strength, which is either the buckling strength, or the plastic strength, that is, the ultimate strength function Γ_u is,

$$\Gamma_u = \Gamma_B \quad \text{or} \quad \Gamma_u = \Gamma_P \tag{9}$$

The assembly of these conditions represents the ultimate strength interaction relationship of the tubular structural unit as shown in **Fig. 3**.

4.3 Elasto-plastic Stiffness Matrix

As the load increases, the ultimate strength condition, for buckling or fully plastic strength, may be satisfied at nodal point i, nodal point j and/or the location of maximum bending moment along the element. The internal force vector at such a location must continue to satisfy Eq. (9). The unit may continue to deform while redistribution of the internal forces takes place, and the ratios of the components of the internal force vector may change. In the following, the stiffness equation of such a structural unit is derived considering three separated cases **(Fig. 4)**.

(a) First, let a structural unit in which Eq. (9) is satisfied at nodal points i or/and j be considered. A plastic node [16] is inserted there. Equation (9) is regarded as a plastic potential and the plastic flow theory is applied.

The incremental form of the stiffness equation is derived as

$$\{dR\} + \{dQ^P\} = [K^P]\,\{dU\} \tag{10}$$

where,

$$[K^P] = [K^e] - [K^e]\,[\Phi]\,([\Phi]^T[K^e]\,[\Phi])^{-1}[\Phi]^T[K^e]$$

$$[\Phi] = [\{\phi_i\}\ \{\phi_j\}]$$

$$\{\phi_i\} = \{\partial\,\Gamma_{pi}/\partial\,\{R\}\},\quad \{\phi_j\} = \{\partial\,\Gamma_{pj}/\partial\,\{R\}\}$$

$\{dQ^P\}$ = elastic-plastic incremental force vector of the distributed load

The explicit form of $[K^P]$ is shown in Appendix II.

(b) If the condition of ultimate strength is satisfied at point a where the position of maximum bending moment occurs along the length of the element, the element is divided at this position into two beam-column elements ia and aj. A plastic node is inserted at point a on either element ia or element aj. Considering the condition of nodal points i and j, elastic or elastic-plastic stiffness matrices and distributed load vectors are evaluated for the two elements. Then the extra nodal displacements at point a are eliminated in the normal way.

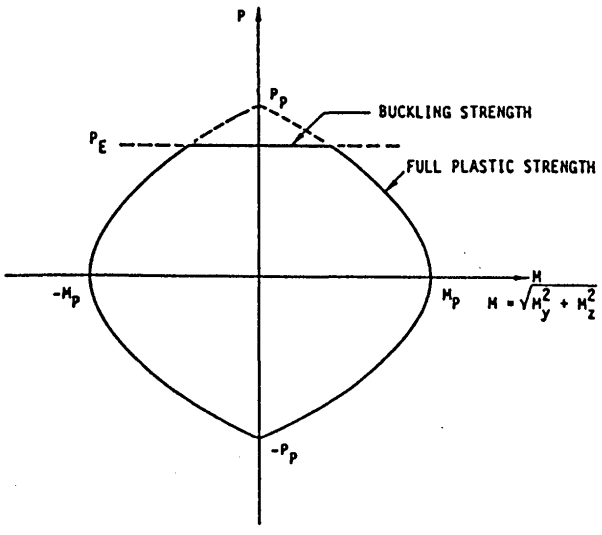

Fig. 3 Ultimate strength interaction relationship.

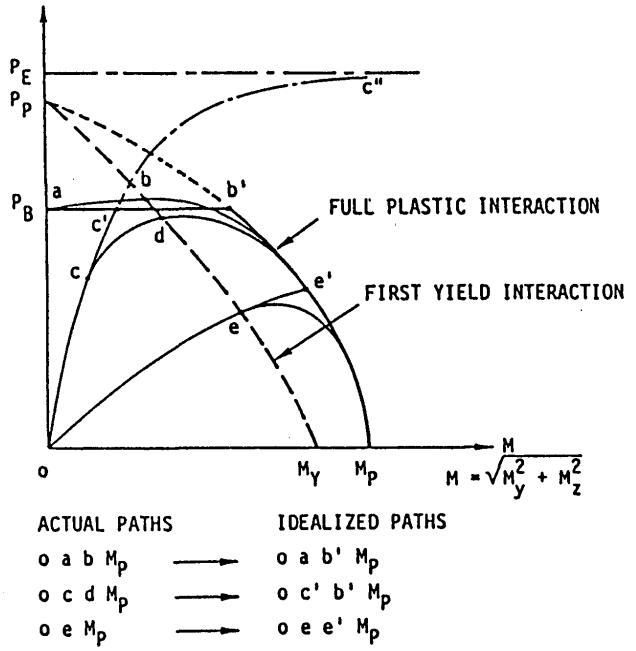

Fig. 4 Idealization of tubular elements.

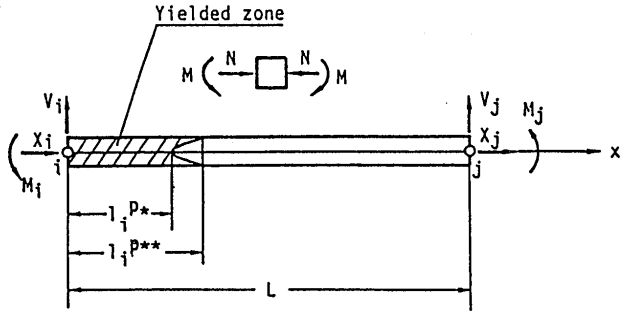

Fig. 5 Structural beam-column element and plastic zone.

(c) If the magnitude of the axial compressive force reaches that of buckling, the element is allowed to buckle. The axial force being maintained at the buckling load, the bending moment increases due to the increase of deflection until Eq. (9) is satisfied at one or both ends and/or any point along the element's length, where a plastic node is then inserted as in (a) and/or (b).

In (b) and (c), the position of maximum bending moment in the middle portion of the element is usually very close to the midlength. In the analysis it may be reasonably assumed at midlength.

4.4 Strain-Hardening Effect (including softening effect)

In deriving K^p mentioned in the preceding section, the material is assumed to be elastic-perfectly plastic. Consequently, the size of the plastic strength function Γ_P does not change, even when the plastic deformation increases. This treatment is satisfactory in most cases. However, the theory has been extended to take into consideration strain-hardening (or softening) effects [35] which may be essential in some cases.

Generalized stress $\{\sigma\}$ and generalized strain $\{\varepsilon\}$ at a cross section of a unit are defined as

$$\{\sigma\} = [N \quad M]^T, \ \{\varepsilon\} = [e \quad K]^T \tag{11}$$

where N and M = axial force and bending moment
e and K = average axial strain and curvature.

Then, introducing the strain-hardening effect, the yield conditon may be expressed as

$$f = Y(\{\sigma\}) - \sigma_0(\bar{\varepsilon}^p) = 0 \tag{12}$$

where Y = yield (fully plastic) function
σ_0 = a parameter expressing the size of the yield surface
$\bar{\varepsilon}^p$ = equivalent plastic strain

Strain-hardening coefficient H_b' for a cross section may be defined as

$$H_b' = d\sigma_0/d\bar{\varepsilon}^p \tag{13}$$

H_b' in the above may be evaluated by integrating the stress and plastic strain distributions in a cross section. The result may be shown as

$$H_b' = H'C\left|A\left(\frac{\partial f}{\partial H}\right)^2 + I\left(\frac{\partial f}{\partial M}\right)\right|^2 \tag{14}$$

where $C = \sigma_0/\{\sigma\}^T\{\partial f/\partial\{\sigma\}\}$

A and I = area and moment of inertia of cross-section

Usually, the plastic region extends not only in the cross-section of node i but also over a length l_iP from node i as illustrated in **Fig. 5**.

When no distributed loads are acting, the plasticity condition at node i is expressed in terms of nodal force $\{X\}$ as

$$\Gamma_{pi} = Y_i(\{X\}) - \sigma_{oi}(\bar{\varepsilon}^p) = 0 \tag{15}$$

Under loading at node i, the following loading condition should be satisfied :

$$d\Gamma_{pi} = \{\phi_i\}^T\{dR\} - H_{bi}'d\bar{\varepsilon}_iP = 0 \tag{16}$$

The stiffness of the element evaluated at plastic node i should be equivalent to that of an element with actual elastic-plastic stress distribution. In other words, the plastic work done in both cases should be the same. From this condition, the strain-hardening coefficient for nodal displacement at i, H_{ni}', may be obtained and the loading condition is rewritten as

$$d\Gamma_{pi} = \{\phi_i\}^T\{dR\} - H_{ni}'d\lambda_i = 0 \tag{17}$$

where $\{\phi_i\}\,d\lambda_i = \{dU^P\}$ = increment of plastic nodal displacement

$$H_{ni}' = H_{bi}'h_i = \frac{H_{bi}'\{R\}^T\{\phi_i\}}{\int \sigma_i(x)g(x)dx}$$

$$g(x) = \frac{H_{bi}'}{H_b'}\frac{\{\partial f/\partial\{\sigma\}\}^T\{d\sigma\}}{\{\partial f_i/\partial\{\sigma_i\}\}^T\{d\sigma_i\}}$$

The loading condition at a plastic node is expressed by Eq. (17) which includes an additional term $H_{ni}'d\lambda_i$ compared with no strain-harding material. Except this, following the same procedure as for elastic perfectly plastic material [16], the incremental stiffness equation is obtained in the form,

$$\{dR\} = [K^P]\{dU\} \tag{18}$$

where $[K^P] = [K^e] - [K^e][\Phi](([H'] + [\Phi]^T[K^e][\Phi])^{-1}[\Phi]^T[K^e]$
$[K^P]$ = elastic-plastic stiffness matrix
$[H']$ = matrix composed of strain-hardening coefficients for nodal displacement

5. Joint Model [26]

In structural analysis of frames, members are usually assumed to be connected rigidly to each other at nodal points. The first step of improvement of this treatment is to introduce a rigid joint model to a joint can so as to maintain the true length of each member for evaluation of the stiffness and locations of plastic hinges.

However, in a tubular frame with simple (unstiffened) joints, the joint may exhibit considerable flexibility in the elastic as well as the elastic-plastic ranges. Some joints may reach their ultimate strength. These may cause excessive deflections and different internal force distribution in the structure. To take these into account, one most conventional method is to use shell finite elements for joint cans and beam elements for the members. This treatment introduces an excessive number of elements and nodes which require enormous modelling and computation time.

In order to overcome this difficulty, in the scope of the "Idealized Structural Unit Method (ISUM)", joint models based on simple elements with elastic-plastic behavior have been developed [26]. Joint models for *T*, *Y*, *TY*, *K*, and *V* joints have been developed. Here, single joint model, for *T* and *Y* joints, is described.

T and *Y* joints are modeled by a group of elements *a*, *b*, and c_T or c_Y as shown in **Fig. 6**. Elements *a* and *b* represent cord and brace respectively and element c_T or c_Y account for wall deformation, exhibiting elastic-plastic behavior. c_T and c_Y are composed of a rigid element and an elastic-plastic element as illustrated in **Fig. 7**. The behavior of a joint model of this type in the plane of the joint (*x-z* plane in **Fig. 6**) is considered, since the out-of-plane loads are usually small. In this model, there are three nodes, *i*, *s* and *j*. External load is applied to node *j* on the brace end and is transmitted to node *i* on the chord center line. Node *s* is an internal node and the stiffness equation of this joint model is expressed as the relationship of nodal forces to nodal displacements at nodes *i* and *j*. This relation is derived in the following way.

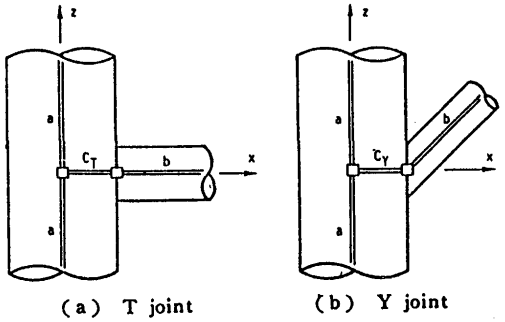

Fig. 6 Modeling T and Y joints by line elements.

Nodal displacement vector $\{U_s\}$ at *s*, is defined in the same way as Eq. (1)

$$\{U_s\} = [u_{xs}\ u_{ys}\ u_{zs}\ \theta_{xs}\ \theta_{ys}\ \theta_{zs}]^T \tag{19}$$

Similarly, nodal force vector $\{R_s\}$ at *s*,

$$\{R_s\} = [P_{xs}\ P_{ys}\ P_{zs}\ M_{xs}\ M_{ys}\ M_{zs}]^T \tag{20}$$

The stiffness equation for the elastic-plastic element is expressed in the elastic range by

$$\begin{Bmatrix} R_s \\ R_j \end{Bmatrix} = \{K_s\} \begin{Bmatrix} U_s \\ U_j \end{Bmatrix} \tag{21}$$

where $[K_s]$ = translational and rotational matrix. whose explicit form is given in Appendix III

As nodal displacement $\{U_s\}$ is transmitted to node *i* by the rigid element, $\{U_s\}$ may be represented in terms of $\{U_i\}$ in the following form.

$$\begin{Bmatrix} U_s \\ U_j \end{Bmatrix} = \begin{bmatrix} [t] & 0 \\ 0 & [I] \end{bmatrix} \begin{Bmatrix} U_i \\ U_j \end{Bmatrix} = [T_s] \begin{Bmatrix} U_i \\ U_j \end{Bmatrix} \tag{22}$$

where, $[t]$ = transformation matrix
$[I]$ = unit matrix

In the same way as with the nodal displacement, the nodal force $\{R_s\}$ is expressed as,

$$\begin{Bmatrix} R_s \\ R_j \end{Bmatrix} = \begin{bmatrix} [t] & 0 \\ 0 & [I] \end{bmatrix} \begin{Bmatrix} R_i \\ R_j \end{Bmatrix} = [T_s] \begin{Bmatrix} R_i \\ R_j \end{Bmatrix} \tag{23}$$

The stiffness equation of the joint element may then be derived as

$$\{R\} = [K]\{U\} \tag{24}$$

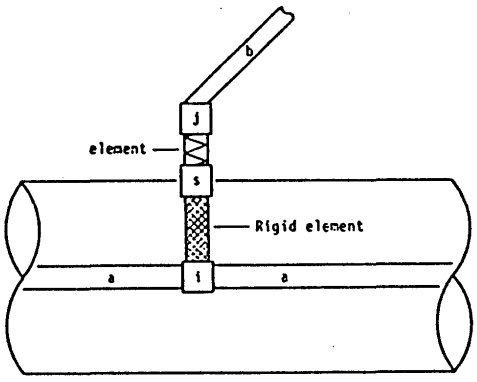

Fig. 7 Idealized "Y joint element".

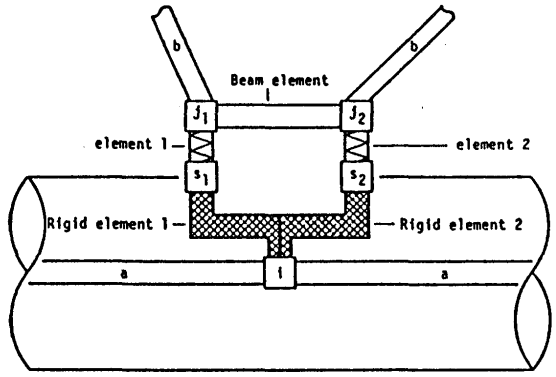

Fig. 8 Idealized "K joint element".

where $\{R\} = [R_i\ R_j]^T$, $\{U\} = [U_i\ U_j]^T$
$[K^e] = [T_s]^T [K_s] [T_s]$ = elastic stiffness matrix

When the components of internal force in element c_T or c_Y satisfy the plasticity condition

$$\Gamma_P = 0 \tag{25}$$

a plastic node is inserted at j and the stiffness equation is expressed in an incremental form as,

$$\{dR\} = [K^P]\ \{dU\} \tag{26}$$

where $[K^P] = [K^e] - [K^e][\Phi]([\Phi][K^e][\Phi])^{-1}[\Phi]^T[K^e]$
$[K^P]$ = elastic-plastic stiffness matrix
H' = strain hardening (softening) coefficient

The explicit form of the matrix is the same as that of case (b) in Appendix II.

In a similar way, a joint model for K joint has been proposed as shown in **Fig. 8**. In this model, in addition to rigid elements and elasto-plastic elements, a beam element is introduced to express the interaction between the two braces.

6. Tubular Element Considering the Influence of Local Denting and Overall Bending Damages

Accidental loads may act on bracing members due to supply boat collisions or objects dropping from platform decks. Such accidental loads lead to local denting and/or overall bending damages. The strength reduction of members due to damage may have serious implications when a structural system is exposed to severe environmental loads before a repair is made. For nonlinear analysis using ISUM, a tubular element considering the influence of bending and denting damage has been proposed [21-23].

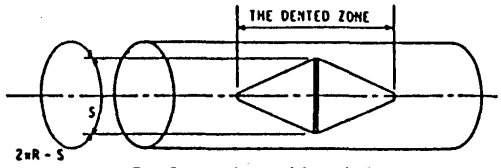

(a) Configuration of local dent

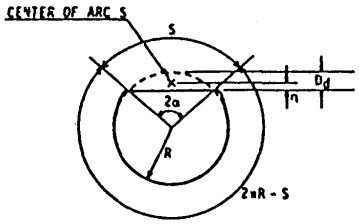

(b) Cross section at bottom of dent

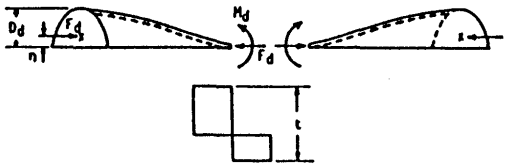

(c) Forces and moments at dented part

Fig. 9 Idealization of local dent.

The configuration of a dent is idealized as in **Fig. 9** [21-22]. The relationship between the force and the bending moment at the flattened bottom part of the dent is expressed as

$$M_d = \eta F_d \tag{27}$$

Introducing the fully plastic condition at the bottom part of the dent, the reduced plastic strength of this part is written in the following form.

$$F_{dp} = D\,\alpha\,\sigma_Y(\sqrt{4\eta^2 + t^2} - 2\eta) \tag{28}$$

In Ref. [23], an empirical coefficient, 80t/D, is multiplied to Eq. (28) to include the effect of D/t ratio. This plastic strength of the dented part may be used to evaluate the full plastic strength function of the cross-section of the element at the dent.

The element is then divided into three regions as shown in **Fig. 10**. Considering the boundary conditions at the nodal points and continuity conditions at the boundaries between these three regions, the relationship between nodal forces and nodal displacements in the elastic state is derived as follows [22].

$$\{R\} = [K^{es}]\ \{U\} + \{L\} + \{C\} \tag{29}$$

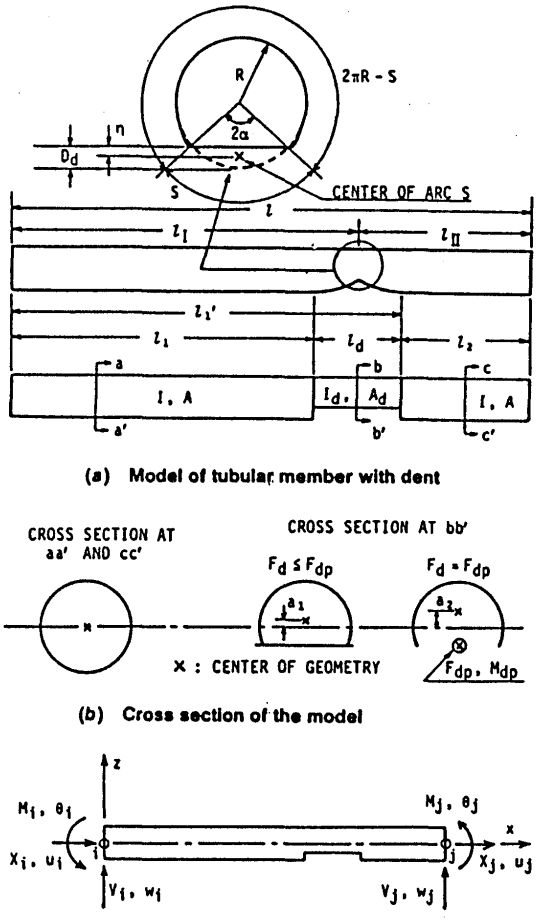

Fig. 10 Model for dented tube.

where $\{R\}$ = nodal forces
$\{K^{es}\}$ = stiffness matrix in a secant form
$\{U\}$ = nodal displacement
$\{L\}$ = equivalent nodal force due to initial deflection
$\{C\}$ = equivalent nodal force due to the eccentricity caused by the dent

The elastic stiffness equation in a tangential form is obtained from Eq. (29).

Performing the overall incremental analysis, the ultimate strength analysis of the dented portion is also performed simultaneously in an analytical manner based on the equilibrium conditions. If the ultimate strength is attained at a certain incremental step, a plastic node [16] is introduced at the middle of the dented part. The analysis hereafter is similar to that of ordinary tubular elements except for the fully plastic strength interaction relationship, which is written as

$$\Gamma_P = M - M_P \cos\left\{\frac{\pi}{2}\left(\frac{P}{P_P} - \frac{F_{dp}}{P_P}\right) + \frac{1}{2}\alpha\right\} + M_P\left[\frac{1}{2}\sin\alpha - \frac{\pi}{2}\frac{F_{dp}}{P_p}\left\{\cos\alpha + \frac{\sin\alpha}{(\pi - \alpha)}\right\}\right] \tag{30}$$

Equation (30) is for the case where the dent bottom line is located perpendicular to the plane of bending, and the dent is in the compression side of bending. The fully plastic strength interaction relationships for general cases are given in Ref. [22] as illustrated in **Fig. 11**.

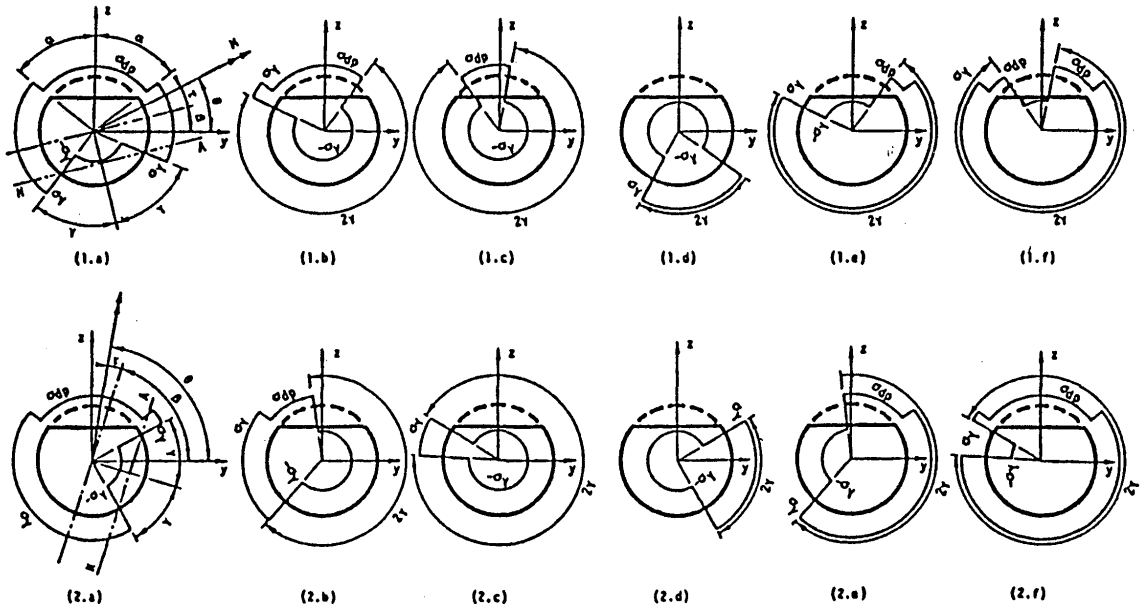

Fig. 11 Fully plastic stress distribution in a dented cross section.

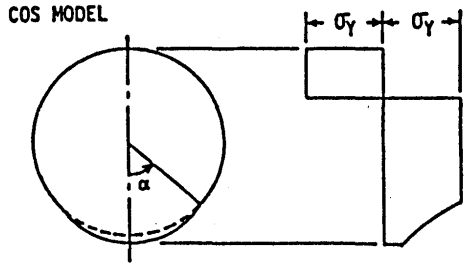

Fig. 12 Fully plastic stress distribution after local buckling.

7. Tubular Element Considering Local Shell Buckling

Tubular bracing members in semi-submersible drilling units have such diameter to thickness ratios that local shell buckling takes place after the ultimate strength of a member has been attained. In order to simulate such behavior, a tubular element has been proposed in Refs. [24, 25].

In the elastic range, the influence of initial deflection in the overall mode is taken into account. The ultimate strength analysis is also performed simultaneously in an analytical manner at the most stressed cross section based on the equilibrium condition. The elastic stiffness equation in an incremental form is the same as Eq. (6). The elastic incremental analysis is continued until the ultimate strength is attained.

The elasto-plastic stiffness matrix is then calculated for this element as in the case of an ordinary tubular element with the necessary modification on the ultimate strength function so as to take account of the effect of local shell buckling. In the elasto-plastic range, the initiation of local shell buckling is checked based on a strain criterion [25]. The strain at the cross section of a plastic node is evaluated with an axial force, P, and a bending moment M related by the following equation.

$$M = M_P \cos\frac{\pi}{2}\frac{P}{P_P} - dM\left(\frac{P}{P_P}\right)^n \tag{31}$$

The part of the cross section at a plastic node where the compressive strain exceeds the critical buckling strain is considered to have locally buckled. The fully plastic stress distribution for this state is illustrated in **Fig. 12**. The fully plastic strength interaction relationship is expressed as

$$\Gamma_P = M - M_d - M_P \cos\left[\frac{\pi}{2}\left(\frac{P}{P_P} - \frac{F_d}{P_P}\right) + \frac{\alpha}{2}\right] + \frac{1}{2}M_P \sin\alpha = 0 \tag{32}$$

where F_d and M_d = the axial force and the bending moment at the locally buckled part

α = half the angle of the buckled part as indicated in **Fig. 12**

α in Eq. (32) is a function of the plastic components of the nodal displacements, u^P, and θ^P. As a result, Eq. (32) reduces to

$$\Gamma_P(P, M, u^P, \theta^P) = 0 \tag{33}$$

The condition to maintain the plastic state is expressed as;

$$d\Gamma_P = \frac{\partial \Gamma_P}{\partial P}dP + \frac{\partial \Gamma_P}{\partial M}dM + \frac{\partial \Gamma_P}{\partial u_P}du + \frac{\partial \Gamma_P}{\partial \theta_P}d\theta = 0 \tag{34}$$

The third and the fourth terms represent the influence of local buckling. The elasto-plastic stiffness matrix is derived from Eq. (34).

Although the parameter n in Eq. (31) may be chosen between 8 and 12, the results of analysis are very close to each other. The post-local buckling behavior is well simulated with this element. The exact estimation of n and the critical local buckling strain remains as a future work.

8. Procedure of Analysis

In the analysis, a structure is divided into the above developed tubular elements and the incremental load method is used. First, the structure free from loading is considered. The incremental stiffness matrix of each element is constructed and transformed into the global coordinates. The global incremental stiffness matrix of the whole structure is then assembled. After the boundary conditions are introduced, the first load increment is applied. The deformation of the structure is obtained and the internal forces in each element are evaluated. Each element is then checked for buckling and/or plastification.

Since the stiffness matrix of the tubular element is dependent on deformation and internal forces, a new stiffness matrix is constructed and transformed into global coordinates for each element after each load increment. The global stiffness matrix is reassembled and the next increment of load is applied.

When buckling and/or plastification of a structural unit or units are detected within a loading step, the load increment is scaled down to that just necessary to cause such failure. This prevents the internal force vectors from shooting out of the ultimate strength interaction surfaces.

The ultimate strength of the structure is detected by consideration of excessive plastic deformation.

Following the procedure outlined in the foregoing, a computer program, NOAMAS, has been completed.

9. Numerical Examples

a) Tubular element

Figure 13 presents examples of comparison among test results of 18 tubular members subjected to axial compression and end bending moments [36], results of elastic plastic large deformation finite element analyses and results obtained using the tubular element of ISUM [19]. In the finite element analyses a member is divided into 8 beam-column elements with large deflection and plastic capabilities. Each elements has 40 integration points along the circumference of the member at the middle of the element. It may be seen that the ISUM element is capable of accurate representation of the behavior of tubular members. Of particular practical interest, loss of stiffness prior to ultimate strength and post-buckling loss of strength are accurately predicted.

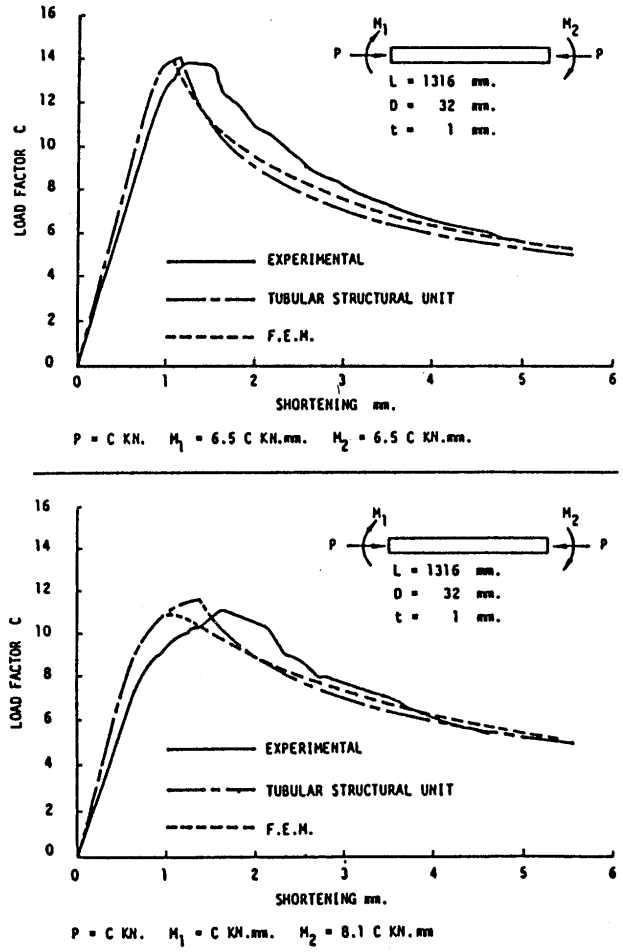

Fig. 13 Comparisons of load-shortening curves of tubular structural units.

b) Strain-hardening effect

Elasto-plastic behavior of a cantilever beam of rectangular cross-section is analysed by the plastic node method and FEM with consideration of strain-hardening effect as indicated in **Fig. 14** [35]. A vertical load P and axial force F are applied proportionally. In the analysis by FEM, the beam is divided into 10 elements in length and 20 layers in depth. From comparison of the results, it is shown that the predicted accurately element has very accurate capability.

c) Tubular element with damages

Figure 15 shows the results of analysis of a damaged tubular column under axial compressive load with eccentricity [23]. Damage is in the form of dent and overall bending. The results are compared with experimental results. The ISUM model is seen to simulate accurately the actual behavior of the test specimen both before and after the ultimate strength. In the axial force-axial strain curve, the unloading and reloading paths are also plotted. These calculations are easily performed by changing only the sign of the load increment. It may be

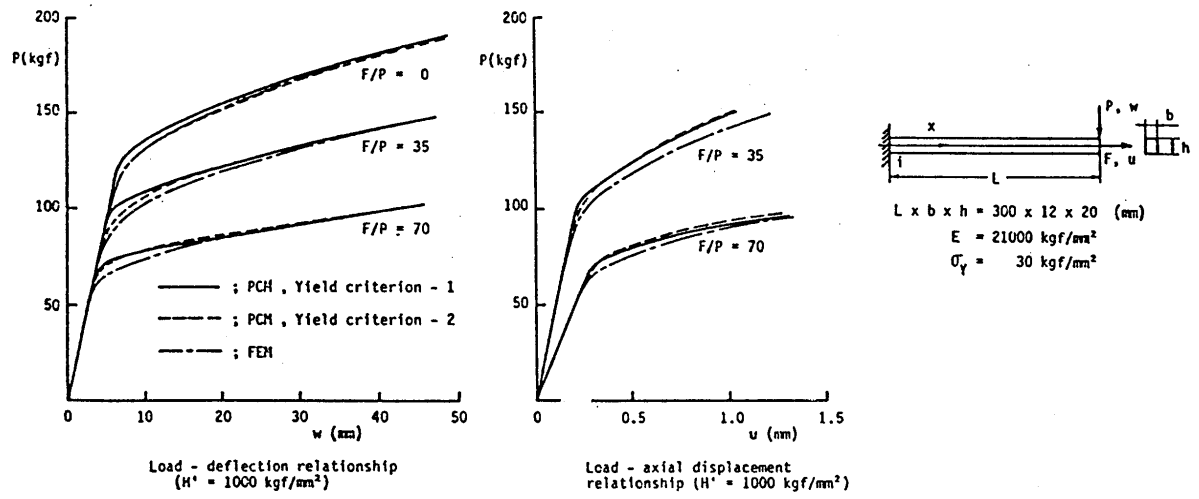

Fig. 14 Elastic-plastic analysis of a cantilever beam under concentrated lateral load and/or axial load at end.

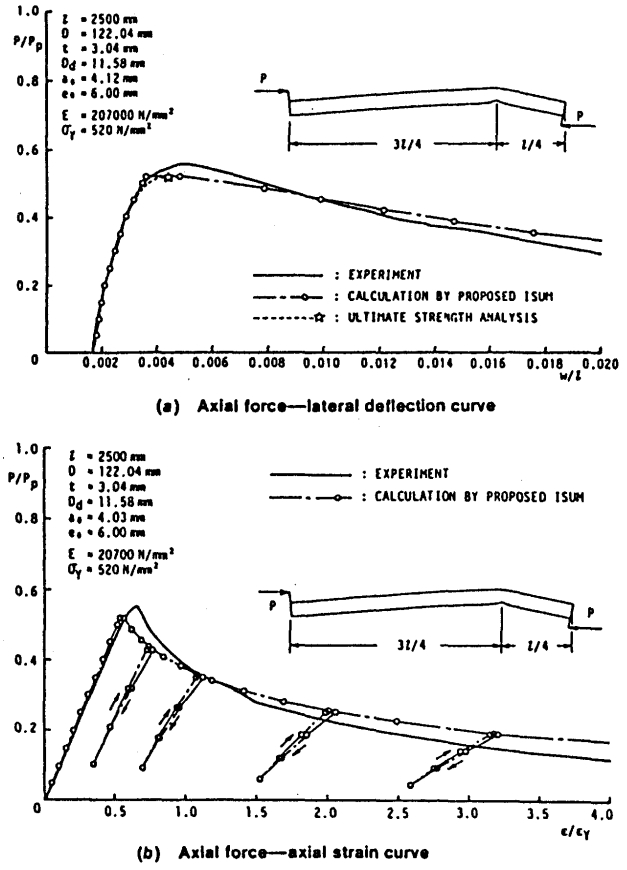

Fig. 15 Behavior of damaged tubular element under axial compression with eccentricity.

seen that this unit is applicable not only for a monotonic loading, but also for cyclic loading and for the overall collapse analysis of a system.

d) Joint models

In order to assess the capability of the present model to represent accurately the nonlinear behavior of actual joints, analysis of the nonlinear behavior of a "K" joint subjected to different loading conditions is carried out using the finite element method (shell model) and the present joint model, and the results are compared to each other. Dimensions and material properties of the "K" joint used in the comparison are shown in **Fig. 16**.

In the analysis by the present model, joint stiffness constants are calculated according to the equations and methods presented in Ref. 26. The yield strength of each individual joint is, however, taken according to finite element results in order to avoid errors involved in the ultimate strength equations available in the literature, and to limit the errors to those due to the modeling itself.

Load-displacement relationships under various loading conditions evaluated by the finite element analysis and those evaluated by the present model are compared and some examples are shown in **Fig. 17**.

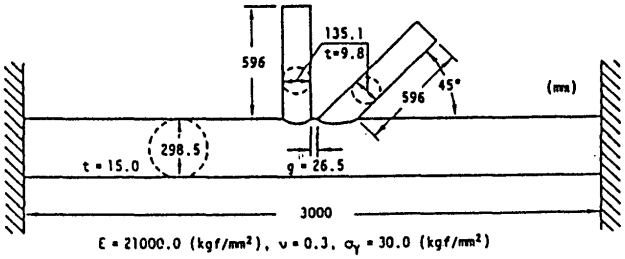

Fig. 16 Dimensions and material properties of K joint.

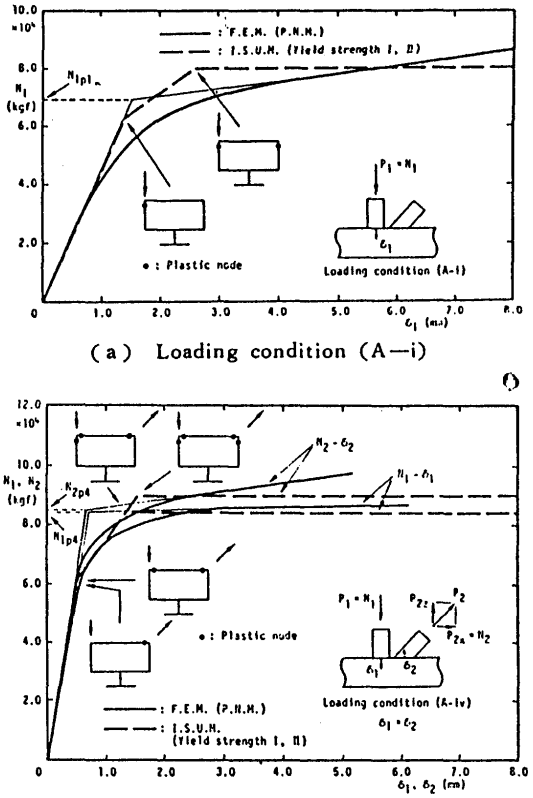

Fig. 17 Local normal load (N)-deflection (δ) relationships of TY joint and behaviors of idealized "TY joint model".

It may be seen that the present model represents the behavior of joints with satisfactory accuracy.

e) Ultimate strength of jack-up rig in survival conditon

A three-legged jack-up rig illustrated in **Fig. 18** is analysed by ISUM. Its particulars are indicated in **Table 1**. Each leg is a lattice structure composed of three chords braced in *K* system and arranged as shown in **Fig. 19**. The rig is designed according to the rules of classification societies to operate in the North Sea.

The rig is fitted with teethed clamps to support vertical forces between the legs and the platform. Tubular elements are used to model the chords and braces while joint elements are used to model joints. The platform

(deck) is considered as a rigid body. The connections of legs to the platform is shown in **Fig. 20**. Clamps are modeled by equivalent springs parallel to the chords of the legs. Leg guides are modeled such that the legs may deform until the clearance between the chords and guide is closed up. Once a chord comes into contact with a guide, relative motion normal to the chord is presented, while friction is not taken into account.

The survival loading condition in waves is considered ; gravity loads, boundary of the legs and wind loads are applied as initial loads and kept constant. The extreme wave load pattern is applied proportionally starting from zero until ultimate strength has been reached. The direction of wind and wave loads are as shown in **Fig. 19** such that the severest condition may be produced in leg A.

Table 1 Principal particulars of jack-up rig

	A RIG
PLATFORM DIMENSION L x B x D (m)	64 x 90 x 9.5
MAX. WATER DEPTH (FEET)	350
WAVE HEIGHT (m)	30.0
CURRENT VELOCITY (m/s)	0.8
WIND VELOCITY (m/s)	45.0
AIR GAP (m)	21.0
LEG PENETRATION (m)	5.0
WIND FORCE (ton)	413
WAVE FORCE (ton)	1,775
O.T.M BY WIND (ton-m)	59,830
O.T.M BY WAVE (ton-m)	154,610
GRAVITY LOAD IN SURVIVAL CONDITION (ton)	16,100
TYPE OF JACKING UNIT	FIXED TYPE + CLAMPING DEVICE
OPERATING SITE	NORTH SEA

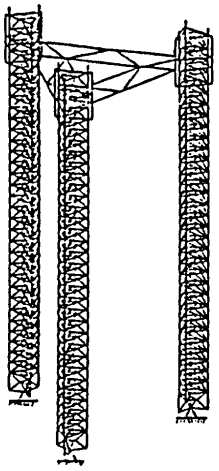

Fig. 18 Calculation model for survival condition.

The relationship between the applied wave load and horizontal displacement of the deck is shown in **Fig. 21**. Initial displacement caused by the initial load may be observed. Failures occur in only one leg, close to the clamps and leg guides. Because of the presence of clamps, which have large stiffness, the bending moments applied on the legs at their connections with the platform are supported directly by axial forces in the leg chords. Forces

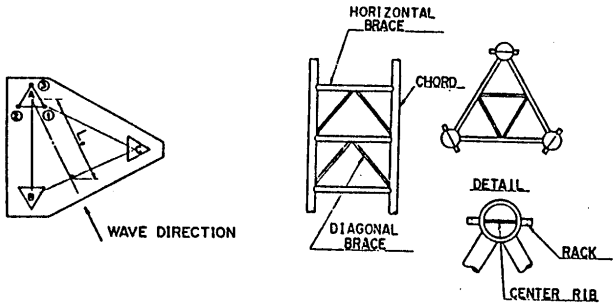

Fig. 19 Arrangement of legs, chords and braces.

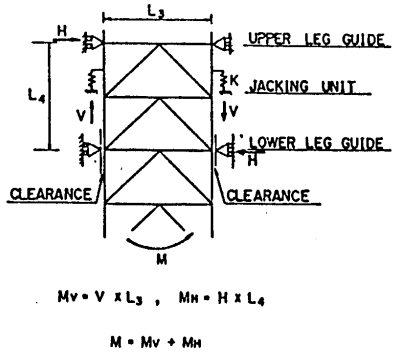

Fig. 20 Reaction forces on jacking units and leg guides.

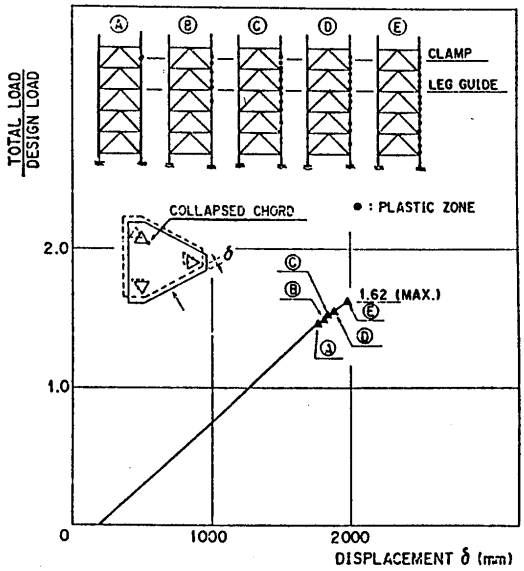

Fig. 21 Ultimate strength in survival condition.

in the braces between the guides do not grow very large while axial forces in the chords continue to increase. Therefore, buckling of the braces is not observed while plastic zone spreads in one leg chord until the rig collapses. Almost no redistribution of internal forces to the other two legs is observed after the first yield until collapse. This indicates that redundancy of the three-legged jack-up rigs is very small.

In this case the collapsed leg may be regarded as a cantilever which collapsed in bending. Ultimate load is found to be 1.62 times the design extreme wave load.

The model has 1953 nodes and 2568 elements. 29 steps are carried out to reach ultimate strength. The analysis requires 6000 seconds of CPU time on a CRAY1 computer to be completed.

10. Summary and Conclusions

In the above, the Idealized Structural Unit Method, ISUM is outlined. Elements used in the analysis of offshore tubular frames are presented, namely, a Tubular element, a Tubular element with strain hardening capability, a Damaged tubular element, a Tubular element with shell buckling capability and Joint elements for *T* and *Y* joint.

Examples of analysis demonstrating the accuracy and efficiency of this method are also presented. It may be seen that this method produces results with accuracy similar to that of a carefully performed FEM analysis while requiring only a small fraction of modelling and computing efforts required by the FEM to analyse similar structures. This makes this method practical for application to actual large size offshore structures.

Acknowledgement

The authors are indebted to Professors T. Yao and M. Fujikubo of Hiroshima University, Japan for their assistance in preparation of this manuscript. They also have made considerable contributions in the development of ISUM and plastic node method.

References

1) Hodge, P. G., *Plastic Analysis of Structures*, McGraw Hill, 1959.
2) H. Okada et al., "Safety Margins for Reliability Analysis of Frame Structures", *Bull. Univ. Osaka Pref.* Ser. A 32-2, 1983.
3) Y. Murotsu et al. , "Reliability Analysis of Frame Structure under Combined Load Effects", *Structural Safety and Rel.*, (ed. by I. Konishi et al.). Vol. I, ICSSAR, 1985.
4) Zayas, V. A., et al., "Inelastic Structural Analysis of Braced Platforms for Seismic Loading", Paper No. *OTC 3979*, 1981.
5) Higginbotham, A. B., "The Inelastic Cyclic Behavior of Axially-Loaded Steel Members", *dissertation*, University of Michigan, Ann Arbor, 1973.
6) Nilforoushan, R., "Seismic Behavior of Multi-story K-Braced Frame Structures", *University of Michigan Research Report UMEE73R9*, Ann Arbor, 1973.
7) Singh, P., "Seismic Behavior of Braces and Braced Steel Frame", *dissertation*, University of Michigan, Ann Arbor, 1977.
8) Marshall, P. W., "Design Considerations for Offshore Structures Having Nonlinear Response to Earthquakes", Preprint, *ASCE Annual Convention and Exposition,* Chicago, 1978.
9) Roeder, C. W. and Popov, E. P., "Inelastic Behavior of Eccentricity Braced Frames Under Cyclic Loading", *EERC Report No. 77-18*, Earthquake Engineering Research Center, University of California, Berkeley, Calif., 1977.
10) Jain, A. K. and Goel, S. C., "Hysteresis Models for Steel Members Subjected to Cyclic Buckling or Cyclic End Moments and Buckling", *University of Michigan Research Report UMEE 78R6*, Ann Arbor, 1978.
11) Maison, B. and Popov, E. P., "Cyclic Response Prediction for Braced Steel Frame", *Journal of the Structural Division*, ASCE, 1980.
12) Ueda, Y. and Rashed, S. M. H., "An Ultimate Transverse Strength Analysis of Ship Structures", *Journal of the Society of Naval Architects of Japan*, Vol. 136, 1974 (In Japanese).
13) Ueda, Y. and Rashed, S. M. H., "The Idealized Structural Unit Method and Its Application to Deep Girder Structures", *Computer and Structures,* Vol. 18, 1984.
14) Ueda, Y., Rashed, S. M. H. and Katayhama, M., "Ultimate Strength Analysis of Double Bottom Structures by Idealized Structural Unit Method", *Journal of Society of Naval Architects of Japan,* Vol. 143, 1987 (In Japanese).
15) Ueda, Y. et al., "A New Theory on Elastic-Plastic Analysis of Framed Structures", *Technology Reports of Osaka University*, Vol. 19, 1969.
16) Ueda, Y. and Yao, T., "The Plastic Node method : A New Method of Plastic Analysis", *Computer Methods in Applied Mechanics and Engineering,* Vol. 34, 1982.
17) Ueda, Y., Rashed, S. M. H. and Paik, J.K., "Plate and Stiffened Plate Units of the Idealized Structural Unit Method (1st Report)", *Jl of Soc. of Naval Architects of Japan,* Vol. 156, 1984 (In Japanese).
18) Ueda, Y., Rashed, S. M. H. and Paik, J.K., "Plate and Stiffened Plate Units of the Idealized Structural Unit Method (2st Report)", *Jl of Soc. of Naval Architects of Japan*, Vol. 159, 1986 (In Japanese).
19) Ueda, Y., Rashed, S. M. H. and Nakacho, K., "New Efficient and Accurate Method of Nonlinear Analysis of Offshore Tubular Frames (The Idealized Structural Unit Method)", *Jl. of Energy Resources Technology,* ASME, Vol. 107, 1985.
20) Rashed, S. M. H., Ishihama, T., Nakacho, K. and Ueda, Y., "Ultimate Strength of Jack-Up Rigs in Survival and Punch-Through Conditions", *Proc. of the 3rd Int. Sym. of Practical Design of Ships and Mobile Units,* Tronheim, 1987.
21) Rashed, S. M. H., "Ultimate Strength and Post-Ultimate Strength Behaviour of Damaged Tubular Structural Members", *Report SK/R52,* Division of Marine Structure, The Norwegian Institute of Technology, 1980.
22) Ueda, Y. and Rashed, S. M. H., "Behavior of Damaged Tubular Structural Members", *Jl of Energy Resources Technology*, ASME, Vol. 107, 1985.
23) Yao, T., Taby, J. and Moan, T., "Ultimate Strength and Post-Ultimate Strength Behavior of Damaged Tubular Members in Offshore Structures", *J. OMAE,* ASME, Vol. 110, 1988.
24) Yao, T., Fujikubo, M., Bai, Y., Nawata, T. and Tamehiro, M., "Local Buckling of Bracing Members in Semi-Submersible Drilling Unit (2nd Report)", *J. Soc. Naval*

Arch. of Japan, Vol. 164, 1988 (In Japanese).
25) Yao, T., Fujikubo, M. and Bai, Y., "Influence of Local Buckling on Behaviour of Tubular Members", *Proc. PRADS*, Vol. 2, 1989.
26) Ueda, Y., Rashed, S. M. H. and Nakacho, K., "An Improved Joint Model and Equations for Flexibility of Tubular Joints", *Proc. of 6th Int. OMAE Symp.*, 1987.
27) Sherman, D. R., "Tests of Circular Tubes in Bending", *Journal of the Structural Division*, ASCE, 1976.
28) Sherman, D. R., Erzurumlu, H. and Mueller, W., "Behavioral Study of Circular Tubular Beam-Columns", *Journal of the Structural Division*, ASCE, 1979.
29) Chen, W. F. and Ross, D. A., "Tests of Fabricated Tubular Columns", *Journal of the Structural Division*, ASCE, 1977.
30) Han, D. J. and Chen, W. F., "Buckling and Cyclic Inelastic Analysis of Steel Tubular Beam-Columns", *Engineering Structures*, Vol. 5, 1983.
31) Bouwkamp, J. G., "Buckling and Post-Buckling Strength of Circular Tubular Sections", *Offshore Technology Conference*, Paper No. OTC 2204, 1975.
32) Chen, W. F. and Atsuta, T., *Theory of Beam-Columns*, Vol. 1, McGraw-Hill Inc., 1976.
33) Bjorhovde, R., "Deterministic and Probabilistic Approaches to the Strength of Steel Columns", *Ph.D. dissertation* in Civil Engineering, Lehigh University, Bethlehem, Pa., 1972.
34) Selberg, A., *Steel Structures*, (in Norwegian), Tapir, Norway, 1972.
35) Ueda, Y. and Fujikubo, M., "Plastic Node Method Considering Strain-hardening Effects", *Jl of Soc. of Naval Architects of Japan*, Vol. 160, 1986 (In Japanese).
36) Kjeoy, H. and Foss, G., "Tests on Buckling Strength and Post Buckling Behavior of Cylindrical Members Subjected to End Moments and Axial Compressive Load", Det Norsk Veritas, *Veritas Report No. 80-0625*, 1980.

Appendix I

EXPRESSIONS FOR NODAL MOMENTS, SHEARING FORCES AND SHORTENING DUE TO BENDING.

In the case where the element is subjected to a linearly distributed load q_m,

$$q_m = q_{mi}[1+(\alpha-1)x/L]$$

$$\alpha = q_{mj}/q_{mi}$$

$$m = y, z$$

1. Nodal moments

$$M_{zi}+M_{zqi}=\frac{P}{a_2}(u_{yi}-u_{yj})+P\frac{a_1+L}{a_2}\theta_{zi}-P\frac{a_1}{a_2}\theta_{zj}$$

$$M_{zj}+M_{zqj}=\frac{P}{a_2}(u_{yi}-u_{yj})-P\frac{a_1}{a_2}\theta_{zi}+P\frac{a_1+L}{a_2}\theta_{zj}$$

$$M_{zqi}=q_{yi}[\frac{1}{2k^2}(2-k^2L\frac{a_1+2L/3}{a_2})-\frac{\alpha L}{2}\frac{a_1L/3}{a_2}]$$

$$M_{zqj}=q_{yi}[\frac{L}{2}\frac{a_1+L/3}{a_2}-\frac{\alpha}{2k^2}(2-k^2L\frac{a_1+2L/3}{a_2})]$$

2. Nodal shearing forces

$$P_{yi}+P_{yqi}=-P_{yj}-P_{yqj}=\frac{P(2-a_2)}{a_2L}(u_{yi}-u_{yj})+\frac{P}{a_2}(\theta_{zi}+\theta_{zj})$$

$$P_{yqi}=q_{yi}[\frac{L}{3}+\frac{\alpha L}{6}+\frac{(1-\alpha)}{2k^2L}(2-\frac{k^2L^2}{3a_2})]$$

$$P_{yqj}=q_{yi}[\frac{\alpha L}{3}+\frac{L}{6}+\frac{(\alpha-1)}{2k^2L}(2-\frac{k^2L^2}{3a_2})]$$

3. Shortening due to bending

$$u_b=\int_0^L(ds-dx)=\frac{1}{2}\int_0^L[(dw_y/dx)^2+(dw_z/dx)^2]dx$$

Introducing the expressions for w_y and w_z into the above equation and performing the integration, u_b may be obtained and expressed as

$$u_b=L[d_1\{(\theta_{yi}+\theta_{yj}+2\phi_z)^2+(\theta_{zi}+\theta_{zj}+2\phi_y)^2\}$$

$$+d_2\{(\theta_{yi}-\theta_{yj})^2+(\theta_{zi}-\theta_{zj})^2\}+(\phi_z^2+\phi_y^2)/2$$

$$+d_3\{q_{zi}(\theta_{yi}+\theta_{yj}+2\phi_z)+q_{yi}(\theta_{zi}+\theta_{zj}+2\phi_y)\}$$

$$+d_4\{q_{zi}(\theta_{yi}-\theta_{yj})+q_{yi}(\theta_{zi}-\theta_{zj})\}$$

$$+d_5(q_{zi}\phi_z+q_{yi}\phi_y)+d_6(q_{zi}^2+q_{yi}^2)]$$

$$d_1=\frac{k^2L^2+kL\sin kL-4(1-\cos kL)}{16(kL\cos\frac{kL}{2}-2\sin\frac{kL}{2})^2}$$

$$d_2=-a_1/8L$$

$$d_3=\frac{1}{2}[(\alpha-1)(\frac{L}{k^2L^2P}-\frac{kL\sin kL}{2(1-\cos kL)-kL\sin kL}\frac{L}{12P})-d_5]$$

$$d_4=\frac{1}{2}[\frac{L}{2P}\frac{\sin kL}{kL(1-\cos kL)}-\frac{1}{k^2LP}]$$

$$(1+\alpha)+d_2\frac{(1+\alpha)L}{P}$$

$$d_5=\frac{L}{12P}(\alpha-1)$$

$$d_6=\frac{L^2}{P^2}(\frac{3\sin kL+kL}{8kL(1-\cos kL)}-\frac{1}{k^2L^2}+\frac{1}{24})$$

$$\phi_z=(u_{zi}-u_{zj})/L$$

$$\phi_y=(u_{yi}-u_{yj})/L$$

$$\alpha=q_{yj}/q_{yi}=q_{zj}/q_{zi}$$

4. Tangential stiffness matrix and distributed load vector

$$K=\eta_0\begin{bmatrix}
1 & \gamma_{1y} & \gamma_{1z} & 0 & -\gamma_{2z} & \gamma_{2y} & -1 & -\gamma_{1y} & -\gamma_{1z} & 0 & -\gamma_{3z} & \gamma_{3y}\\
 & \eta_1+\gamma_{1y}^2 & \gamma_{1y}\gamma_{1z} & 0 & -\gamma_{1y}\gamma_{2z} & \eta_3+\gamma_{1y}\gamma_{2y} & -\gamma_{1y} & -\eta_1-\gamma_{1y}^2 & -\gamma_{1y}\gamma_{1z} & 0 & -\gamma_{1y}\gamma_{3z} & \eta_3+\gamma_{1y}\gamma_{3y}\\
 & & \eta_1+\gamma_{1z}^2 & 0 & -\eta_3-\gamma_{1z}\gamma_{2z} & \gamma_{1z}\gamma_{2y} & -\gamma_{1z} & -\gamma_{1z}\gamma_{1y} & -\eta_1-\gamma_{1z}^2 & 0 & -\eta_3-\gamma_{1z}\gamma_{3z} & \gamma_{1z}\gamma_{3y}\\
 & & & \eta_5 & 0 & 0 & 0 & 0 & 0 & -\eta_5 & 0 & 0\\
 & & & & \eta_2+\gamma_{2z}^2 & -\gamma_{2z}\gamma_{2y} & \gamma_{2z} & \gamma_{2z}\gamma_{1y} & \eta_3+\gamma_{2z}\gamma_{1z} & 0 & \eta_4+\gamma_{2z}\gamma_{3z} & -\gamma_{2z}\gamma_{3y}\\
 & & & & & \eta_2+\gamma_{2y}^2 & -\gamma_{2y} & -\eta_3-\gamma_{2y}\gamma_{1y} & \gamma_{2y}\gamma_{1z} & 0 & -\gamma_{2y}\gamma_{3z} & \eta_4+\gamma_{2y}\gamma_{3y}\\
 & & & & & & 1 & \gamma_{1y} & \gamma_{1z} & 0 & \gamma_{3z} & -\gamma_{3y}\\
 & & & & & & & \eta_1+\gamma_{1y}^2 & \gamma_{1y}\gamma_{1z} & 0 & \gamma_{1y}\gamma_{3z} & -\eta_3-\gamma_{1y}\gamma_{3y}\\
 & & & & SYM. & & & & \eta_1+\gamma_{1z}^2 & 0 & \eta_3+\gamma_{1z}\gamma_{3z} & -\gamma_{1z}\gamma_{3y}\\
 & & & & & & & & & \eta_5 & 0 & 0\\
 & & & & & & & & & & \eta_2+\gamma_{3z}^2 & -\gamma_{3z}\gamma_{3y}\\
 & & & & & & & & & & & \eta_2+\gamma_{3y}^2
\end{bmatrix}$$

$$\Delta Q=\begin{Bmatrix}
\Delta q_{yi}g_y+\Delta q_{zi}g_z\\
\Delta q_{yi}(f_1+\gamma_{1y}g_y^1)\\
\Delta q_{zi}(f_1+\gamma_{1z}g_y^1)\\
0\\
-\Delta q_{zi}(f_2+\gamma_{2z}g_z^1)\\
\Delta q_{yi}(f_2+\gamma_{2y}g_y^1)\\
-\Delta q_{yi}g_y-\Delta q_{zi}g_z\\
\Delta q_{yi}(f_3+\gamma_{1y}g_y^1)\\
\Delta q_{zi}(f_3+\gamma_{1z}g_z^1)\\
0\\
-\Delta q_{zi}(f_4+\gamma_{3z}g_z^1)\\
\Delta q_{yi}(f_4+\gamma_{3y}g_y^1)
\end{Bmatrix}$$

$\eta_0=EA/Le$

$\eta_1=P(2-a_2)/a_2L\,\eta_0$

$\eta_2=P(a_1+L)/a_2\,\eta_0$

$\eta_3=P/a_2\,\eta_0$

$\eta_4=-Pa_1/a_2\,\eta_0$

$\eta_5=Gj/L\,\eta_0$

$a_1=(\sin KL-kL)/(1-\cos kL)$

$a_2=2[(kL\sin kL)/(1-\cos kL)]$

$$\gamma_{1n}=\frac{d\eta_1\eta_0}{dP}L\phi_n+\frac{d\eta_3\eta_0}{dP}(\theta_{mi}+\theta_{mj})-q_{ni}\frac{df_1}{dP}$$

$$\gamma_{2n}=\frac{d\eta_3\eta_0}{dP}L\phi_n+\frac{d\eta_2\eta_0}{dP}\theta_{mi}+\frac{d\eta_4\eta_0}{dP}\theta_{mj}-q_{ni}\frac{df_2}{dP}$$

$$\gamma_{3n}=\frac{d\eta_3\eta_0}{dP}L\phi_n+\frac{d\eta\ \eta_0}{dP}\theta_{mj}+\frac{d\eta_4\eta_0}{dP}\theta_{mi}-q_{ni}\frac{df_4}{dP}$$

$$f_1=\frac{L}{3}+\frac{\alpha L}{6}+(1-\alpha)\frac{1}{2k^2L}\left(2-\frac{k^2L^2}{3a_2}\right)$$

$$f_2=\frac{1}{2k^2}\left(2-k^2L\frac{a_1+2L/3}{a_2}\right)-\frac{\alpha L}{2}\frac{a_1+L/3}{a_2}$$

$$f_3=\frac{\alpha L}{3}+\frac{L}{6}+(\alpha-1)\frac{1}{2k^2L}\left(2-\frac{k^2L^2}{3a_2}\right)$$

$$f_4=\frac{L}{2}\frac{a_1+L/3}{a_2}-\frac{\alpha}{2k^2}\left(2-k^2L\frac{a_1+2L/3}{a_2}\right)$$

$$g_n=[d_3(\theta_{mi}+\theta_{mj}+2\phi_n)+d_4(\theta_{mi}+\theta_{mj})+d_5\phi_n+2d_6q_{ni}]/e$$

$$g_n^1=(\Delta q_{yi}g_y+\Delta q_{zi}g_z)/\Delta q_{ni}$$

$$e=[1+EA(b_{y1}+b_{z1})]$$

$$b_{n1}=\frac{dd_1}{dP}(\theta_{mi}+\theta_{mj}+2\phi_n)^2+\frac{dd_2}{dP}(\theta_{mi}-\theta_{mj})^2+\frac{dd_3}{dP}q_{ni}(\theta_{mi}+\theta_{mj}+2\phi_n)+\frac{dd_4}{dP}q_{ni}(\theta_{mi}-\theta_{mj})+\frac{dd_5}{dP}q_{ni}\phi_n+\frac{dd_6}{dP}q_{ni}^2$$

$$\phi_n=(u_{ni}-u_{nj})/L$$

$m=y,\ z \qquad n=z,\ y$

Appendix II

EXPLICIT FORMS OF THE ELASTIC-PLASTIC STIFFNESS MATRIX AND INCREMENTAL DISTRIBUTED LOAD VECTOR

a. End i plastic and end j elastic.

$$K^p=\begin{bmatrix}
K_{ii}-K_{ii}\phi_i\phi_i^TK_{ii}/A_1 & K_{ij}-K_{ii}\phi_i\phi_i^TK_{ji}/A_1\\
K_{ji}-K_{ji}\phi_i\phi_i^TK_{ii}/A_1 & K_{jj}-K_{ji}\phi_i\phi_i^TK_{ij}/A_1
\end{bmatrix}$$

$$\Delta Q^P=\begin{Bmatrix}
\Delta Q_i-(B_1/A_1)K_{ii}\phi_i\\
\phi Q_j-(B_1/A_1)K_{ji}\phi_i
\end{Bmatrix}$$

$A_1=\phi_i^TK_{ii}\phi_i \qquad B_1=\phi_i^T\Delta Q_i$

b. End i elastic and end j plastic.

$$K^p=\begin{bmatrix}
K_{ii}-K_{ij}\phi_j\phi_j^TK_{ji}/A_2 & K_{ij}-K_{ij}\phi_j\phi_j^TK_{jj}/A_2\\
K_{ji}-K_{jj}\phi_j\phi_j^TK_{ji}/A_2 & K_{jj}-K_{jj}\phi_j\phi_j^TK_{jj}/A_2
\end{bmatrix}$$

$$\Delta Q^P=\begin{Bmatrix} \Delta Q_i-(B_2/A_2)K_{ij}\phi_j \\ \phi Q_j-(B_2/A_2)K_{jj}\phi_j \end{Bmatrix}$$

$$A_2=\phi_j^T K_{jj}\phi_j \qquad B_2=\phi_j^T \Delta Q_j$$

c. Both sides plastic.

$$K^P=\begin{bmatrix} K_{ii} & K_{ij} \\ K_{ji} & K_{jj} \end{bmatrix}-\frac{1}{A}\begin{bmatrix} K_{ii}\phi_i & K_{ij}\phi_j \\ K_{ji}\phi_i & K_{jj}\phi_j \end{bmatrix} G$$

$$G=\begin{bmatrix} A_2\phi_i^T K_{ii}-A_{12}\phi_j^T K_{ji} & A_2\phi_i^T K_{ij}-A_{12}\phi_j^T K_{jj} \\ A_1\phi_j^T K_{ji}-A_{21}\phi_i^T K_{ii} & A_1\phi_j^T K_{jj}-A_{21}\phi_i^T K_{ij} \end{bmatrix}$$

$$\Delta Q^P=\begin{Bmatrix} \Delta Q_1-\frac{1}{A}[A_2B_1-A_{12}B_2)K_{ii}\phi_i+(A_1B_2-A_{21}B_1)K_{ij}\phi_j] \\ \Delta Q_j-\frac{1}{A}[(A_2B_1-A_{12}B_2)K_{ji}\phi_i+(A_1B_2-A_{21}B_1)K_{jj}\phi_j] \end{Bmatrix}$$

$$A_{12}=\phi_i^T K_{ij}\phi_j$$

$$A_{21}=\phi_j^T K_{ji}\phi_i$$

$$A=A_1A_2-A_{12}A_{21}$$

Appendix III

$$[K_s]=\begin{bmatrix} k_x & & & & & & -K_x & & & & & \\ & k_y & & & & & & -K_y & & & 0 & \\ & & k_z & & & & & & -K_z & & & \\ & & & k_{mx} & & & & & & -k_{mx} & & \\ & & & & k_{my} & & 0 & & & & -k_{my} & \\ & & & & & k_{mz} & & & & & & -k_{mz} \\ & & & & & & k_x & & & & & \\ & & & & & & & k_y & & & & \\ & & & & & & & & k_z & & & \\ & & & SYM. & & & & & & k_{mx} & & \\ & & & & & & & & & & k_{my} & \\ & & & & & & & & & & & k_{mz} \end{bmatrix}$$

where k_x, k_y, k_z, k_{mx}, k_{my}, and k_{mz} are stiffness constants in three translational and rotational directions.